



# Phase diagram and dielectric properties of mixed $\text{Cs}_{1-x}(\text{NH}_4)_x\text{H}_2\text{PO}_4$ crystals

Authors: A. I. Baranov, V. V. Dolbinina, S. Lancers-Mendez, and V. Hugo Schmidt

This is an Accepted Manuscript of an article published in [Ferroelectrics](#) in 2002, available online: <https://www.tandfonline.com/10.1080/00150190211553>.

A.I. Baranov, V.V. Dolbinina, S. Lancers-Mendez, and V.H. Schmidt, "Phase diagram and dielectric properties of mixed  $\text{Cs}_{1-x}(\text{NH}_4)_x\text{H}_2\text{PO}_4$  crystals," *Ferroelectrics* 272, 225-230 (2002). doi: 10.1080/00150190211553.

Made available through Montana State University's [ScholarWorks](#)  
[scholarworks.montana.edu](http://scholarworks.montana.edu)

## PHASE DIAGRAM AND DIELECTRIC PROPERTIES OF MIXED $\text{Cs}_{1-x}(\text{NH}_4)_x\text{H}_2\text{PO}_4$ CRYSTALS

A.I. BARANOV<sup>a)</sup>, V.V. DOLBININA<sup>a)</sup>,  
S. LANCEROS-MENDEZ<sup>b)</sup> and V.H. SCHMIDT<sup>c)</sup>

<sup>a)</sup>Institute of Crystallography of RAS, 117333 Moscow, Russia

<sup>b)</sup>Universidade do Minho, 4710 Braga, Portugal

<sup>c)</sup>Montana State University, Bozeman, MT 59717, USA

*(Received in final form November 24, 2001)*

Influence of  $\text{NH}_4 \rightarrow \text{Cs}$  substitution has been studied in the mixed  $\text{Cs}_{1-x}(\text{NH}_4)_x\text{H}_2\text{PO}_4$  crystals system by means of dielectric measurements. The x-T phase diagram was determined: for ammonium concentrations up to 0.1 the system has a monoclinic paraelectric phase with a transition into a ferroelectric phase whose temperature increases with increasing ammonium concentration. For ammonium concentration 0.4 to 1.0 the system shows a tetragonal paraelectric phase and a transition into an antiferroelectric phase. No solid solutions with concentrations between 0.1 and 0.4 could be grown. The system was further studied with the quasi-one-dimensional Ising model and the three-dimensional anisotropic Ising model.

Keywords: mixed crystals; dielectric; quasi-one-dimensional; KDP; CDP

### INTRODUCTION

In the mixed crystals of the KDP family the glass state forms due to the competition of antiferroelectric (AFE) and ferroelectric (FE) interactions<sup>[1]</sup>. In the present work, the influence of the  $\text{Cs} \rightarrow \text{NH}_4$  cation substitution on the phase transition and the possible formation of a glass state were studied in mixed  $\text{Cs}_{1-x}(\text{NH}_4)_x\text{H}_2\text{PO}_4$  (CADP) crystals with  $0 \leq x \leq 1$ . Two main points of interest make this system different from the other mixed crystals in the KDP family: on the one hand we will study the effects of the substitutional impurities on the ferroelectric properties of the quasi-one-dimensional  $\text{CsH}_2\text{PO}_4$  <sup>[2-4]</sup>. On the other hand, the ionic radii of  $\text{Cs}^+$  and  $\text{NH}_4^+$  are quite different and the pure

crystals,  $\text{NH}_4\text{H}_2\text{PO}_4$  (ADP) and  $\text{CsH}_2\text{PO}_4$  (CDP), belong to different crystalline structures: tetragonal and monoclinic, respectively.

## EXPERIMENTAL

CADP single crystals were grown from water solutions by the slow evaporation method. The concentration in the solid solutions was determined by direct chemical analysis. The auto-balanced Quad Tech 7600 Precision RLC Meter and Tesla BM-595 bridge were used for measurements of the complex dielectric constant in the frequency range 10 Hz - 1 MHz. A closed cycle helium cryostat (Janis Research Co., Inc. Model C210) was used in temperature range 15-350 K. Samples in the form of rectangular plates ( $0.5 \times 0.5 \times 0.1$  cm<sup>3</sup>) were oriented along the crystallographic axes. Mixed sputtered Au-Pd as well as silver paint electrodes were used.

## RESULTS AND DISCUSSION

### Phase Diagram

For mixed CADP crystals the monoclinic modification grows from water solutions with ammonium concentrations  $0 < x < 0.35$ . At higher concentrations ( $0.35 < x < 1$ ) only crystals in the tetragonal modification grow. Both, monoclinic and tetragonal modifications of CADP (with concentrations in crystal  $x=0.09$  and  $0.4$ , respectively) grow from water solution with  $x \approx 0.35$ . The ammonium concentration in the crystals differs significantly from that in the aqueous solutions and varies between 0 and 0.09 in the monoclinic modification and between 0.4 and 1 in the tetragonal modification. Thus, mixed CADP crystals do not form in the concentration ranges  $0.09 < x < 0.4$ .

The temperature dependences of the dielectric permittivity of monoclinic CADP measured along the FE *b*-axes and tetragonal CADP measured perpendicular to the tetragonal *c*-axes is shown in Fig. 1,2.

The temperature of the FE phase transition of monoclinic CADP monotonically increases from 154.5 K to 175 K with increasing *x*. The peak of dielectric permittivity  $\epsilon_0$  slightly smears out when *x* increases and its value at  $T_c$ ,  $\epsilon_{b\max}$ , decreases from  $3 \cdot 10^5$  in pure CDP down to  $2 \cdot 10^4$  for CADP with  $x=0.1$ . At  $x \geq 0.3$  the temperature of  $\epsilon_{b\max}$  becomes frequency dependent.

The shape of the dielectric hysteresis loops do not change with increasing *x* and only an increase in the coercive field is observed. The

saturated spontaneous polarization in monoclinic CADP slightly increases with increasing  $x$  (about 20-30%).

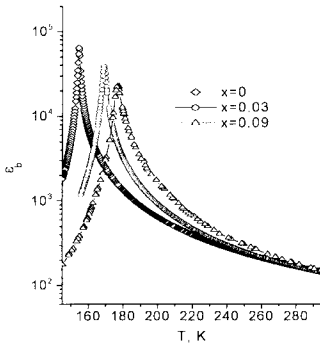


FIGURE 1  $\epsilon_b(T)$  for monoclinic CADP with  $x=0, 0.03, 0.09$  measured at frequency 1 MHz.

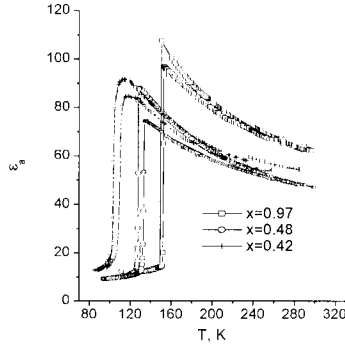


FIGURE 2  $\epsilon_a(T)$  for tetragonal CADP with  $x=0.42, 0.47$  and  $0.97$  measured at frequency 1 MHz.

In the tetragonal CADP crystals with  $x > 0.5$  the temperature behavior of  $\epsilon_a$  and  $\epsilon_c$  practically does not depend on  $x$  and the step-like anomalies of  $\epsilon_a(T)$  and  $\epsilon_c(T)$  at  $T_N$  shift to *lower* temperatures with decreasing  $x$  (Fig.2). For  $x < 0.5$  a broad cusp arises instead of the step-like anomaly, characteristic of smearing out the AFE phase transition. However, the low-frequency dispersion indicative of glass - like behavior does not appear in the vicinity of  $T_N$  down to the lowest ammonium concentrations ( $x=0.4$ ) corresponding to tetragonal modification. The temperature hysteresis increases with decreasing  $x$  and it reaches the value 10 K for CADP 0.4.

The  $xT$ -phase diagram of CADP (Fig.3) was plotted based on the phase transition temperatures  $T_c$  and  $T_N$ , determined from dielectric data. The concentration dependences of both  $T_c$  (in monoclinic CADP) and  $T_N$  (in tetragonal CDP) are nonlinear. On the cesium rich side the unusual result is the increasing of  $T_c$  when  $x$  increases. Moreover, the initial slope of this dependence is anomalously large;  $dT_c/dx = 780$  deg. For comparison, the initial slope in  $Cs(H_{1-x}D_x)_2PO_4$  is  $115$  deg<sup>[4]</sup>.

It is interesting to note that on the ammonium rich side large Cs concentration ( $\approx 40\%$ ) do not seem to modify the principal features of the AF transition, whereas in RADP, KADP and RADA at  $x \geq 30\%$  the glass phase occurs<sup>[1]</sup>.

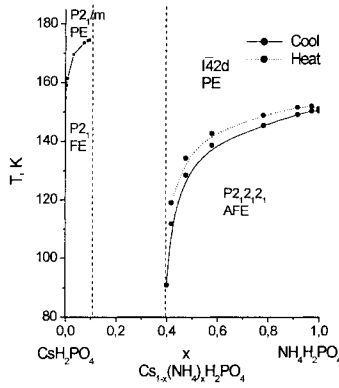


FIGURE 3.  $xT$ -phase diagram of  $Cs_{1-x}(NH_4)_xH_2PO_4$ .

### Critical Behavior of the Static Permittivity in Monoclinic CADP

The critical behavior of CDP is usually described in the terms of the quasi-1d Ising model (eq. (1)) or the three-dimensional anisotropic Ising model (eq. (2))<sup>[2]</sup>

$$\varepsilon_b = \varepsilon_{b\infty} + \frac{C}{T \exp\left(-\frac{2J_{||}}{T}\right) - J_{\perp}} \quad (1); \quad \varepsilon_b = \varepsilon_{b\infty} + \frac{A}{(T - T_0)^\gamma} \quad (2)$$

The analysis of the critical behavior of  $\varepsilon_b$  in CADP is complicated by the influence of the high temperature conductivity ( $T > 250$  K) and the effect of the electrodes. These facts explain the large difference of the parameters in eqs. (1,2) found in the literature<sup>[2-4]</sup>. Our results point out that an increase of the temperature range to high temperature and a decrease of the measuring frequency lead to an increase of  $C$  and  $A$  in eqs. (1, 2). An increase of  $\gamma$  due to an additional contribution of hopping conductivity to the complex permittivity is also observed. The fitting of the experimental points close to  $T_c$  decreases  $J_{||}$  and increases  $J_{\perp}$ . The neglect of  $\varepsilon_{b\infty}$  increases  $C, A$  and  $J_{\perp}$ , but decreases  $J_{||}$  and  $\gamma$ . At  $T > 250$  K the static dielectric constant  $\varepsilon_{b_s}$  was calculated as the high-frequency limit of  $\varepsilon_b(\nu)$  and it is close to that measured at the frequency 1 MHz. At  $T > 330$  K the difference between  $\varepsilon_b(1 \text{ MHz})$  and  $\varepsilon_{b_s}$  increases exponentially. So, the dielectric data at fixed frequency  $\nu = 1 \text{ MHz}$  gives the best fit only below 330 K.

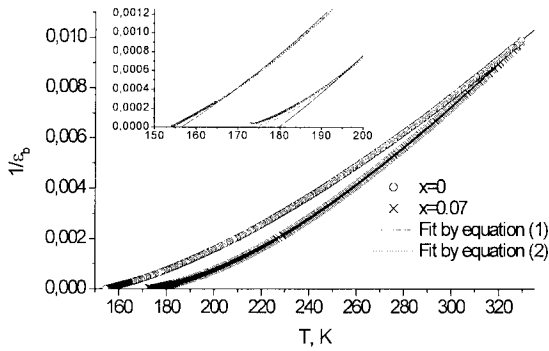


FIGURE 4 Temperature dependence of inverse dielectric permittivity  $1/\epsilon_b$  in CDP and CADP with  $x=0.07$ . The solid and dotted lines are the fittings by eqs.(1) and (2).

In order to avoid errors due to the dielectric dispersion in the vicinity of  $T_c$ , the low temperature limit of the fitting must be restricted  $T=T_c+15$  K. Figure 4 shows the best fitting results with eqs. (1, 2) for pure CDP with  $\epsilon_{\infty} = 8$  and other free parameters. The results for  $C, J_{\parallel}, J_{\perp}$  are similar to the ones found in the literature. The results of the nonlinear curve fitting depend on the details of the fitting procedure because the parameters in eqs. (1,2) are mutually dependent.

CADP	$C/K$	$J_{\parallel}/K$	$J_{\perp}/K$	$\gamma$
$x=0.00$	5224	294.6	2.91	1.36
$x=0.03$	3645	305.5	5.02	1.40
$x=0.07$	2921	339.7	4.16	1.48
$x=0.09$	3033	364.0	3.25	1.52

TABLE I Fitting parameters of the quasi-one-dimensional Ising model and the exponent  $\gamma$  of the three-dimensional anisotropic Ising model for different CADP compositions.

Figure 4 shows the fit of the experimental data eqs (1, 2). An increasing of  $J_{\parallel}$  with increasing  $x$  is observed (Table I). The initial slope of the  $J_{\parallel}(x)$  dependence is estimated as  $dJ_{\parallel}/dx \approx 2000 \pm 500$ . On the other hand,  $J_{\perp}$  decreases when  $x$  increases. As a result, the anisotropy of the interaction ( $J_{\parallel}/J_{\perp}$ ) increases with increasing  $x$ . The

Curie constant  $C$  decreases by a factor 0.44-0.55 when  $x$  increases from 0 to 0.1, instead of increasing proportionally to  $P_s^2$ . This suggests that equation (1) is not correct, probably because of the omission of the proton tunneling. The three-dimensional Ising model seems to describe better the behavior of the crystals, especially in the temperature region close to the transition point (Fig. 4). Nevertheless, the same problem with the Curie constant is observed. The parameter  $\gamma$  has the tendency of increasing with increasing  $x$  (Table I), as it was also observed for CDP upon deuteration<sup>[4]</sup> and substitution  $Cs \rightarrow Tl$ <sup>[5]</sup>.

A possible explanation of the failure of the quasi-one-dimensional model is a crossover between a non-interacting random local temperature defect region and interacting defect region due to the increase in the correlation length along the  $b$ -axis when temperature approaches to  $T_c$ .

## CONCLUSION

The CADP phase diagram shows an opposite influence of the  $Cs \rightarrow NH_4$  and  $NH_4 \rightarrow Cs$  substitutions on the phase transition temperature of the monoclinic and tetragonal modifications. No indications of the glass state were found. The quasi-1d-Ising model has to be improved in order to take into account the peculiarities of the monoclinic CADP crystal system. The 3d-anisotropic Ising model seems to better fit the system, especially in the region close to the transition point.

## ACKNOWLEDGEMENTS

Dr. S.C. Meschia is gratefully acknowledged for assistance with dielectric measurements and Dr. E. Efremova for chemical analysis. Financial support was provided from NSF Grant DMR-9805272 and RFBR Grant 99-02-17443.

## REFERENCES

- [1.] V. H. Schmidt, *Ferroelectrics*, **72**, 157 (1987)
- [2.] R Blinc, B. Zeks, A. Levstic, C. Filipic, J. Slak, M Bugar, I Zupanic, L.A. Shuvalov and A.I. Baranov, *Phys. Rev. Lett.* **38**, 1299 (1977)
- [3.] B.C. Frazer, D. Semmingsen, W.D. Ellenson and G. Shirane, *Phys. Rev. B*, **20**, 2745 (1979)
- [4.] K. Deguchi, E. Okaue and E. Nakamura, *J. Phys. Soc. Jpn.*, **51**, 3569 (1982)
- [5.] J.-H. Ko and J.-J. Kim, *J. Phys.: Condens. Matter*, **11**, 299 (1999), and references therein.